Conformational Analysis of Apparicine using ^{1}H Nuclear Magnetic Relaxation: Application of Transient Nuclear Overhauser Enhancements

By **Frank Heatley,* Lalarukh Akhter,** and **Richard T. Brown,** Chemistry Department, University of Manchester, Manchester M13 9PL

^{1}H N.m.r. relaxation in apparicine in [$^2H_6$]acetone solution has been studied. Spin–lattice relaxation times, and selected steady-state and transient nuclear Overhauser enhancements are reported. In conjunction with spin–spin coupling constants these results permit an assignment of the molecular conformation.

^{1}H N.M.R. data for 10-methoxyapparicine (2) isolated from leaves of *Ochrosia oppositifolia* have been published in a previous note.[1] The observation of a nuclear Overhauser enhancement of 10% for H-15 in 10-hydroxyapparicine (3) on irradiation of the 18-methyl signal led to the assignment of the *E* configuration for C-19 shown in the structural diagram.

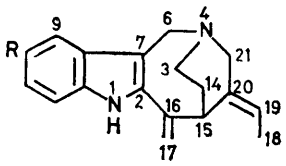

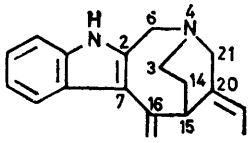

(1) R = H
(2) R = OMe
(3) R = OH

(4)

In this paper, we report an extensive ^{1}H magnetic relaxation study of apparicine [2] (1), carried out with the objectives of assigning all protons unambiguously and elucidating the molecular conformation. It has also conclusively eliminated the alternative structure (4), which is biogenetically unlikely but still compatible with previously available evidence. Three types of relaxation experiment have been performed. First, spin–lattice relaxation times (T_1) of all peaks have been measured using the well known non-selective inversion recovery sequence, *i.e.* all signals were inverted simultaneously. Secondly, selected steady-state nuclear Overhauser enhancements (NOEs) have been measured, whereby the enhancement of a signal consequent on continuous saturation of another signal is monitored. Thirdly, a number of transient NOEs [3,4] have been measured, whereby the transient enhancement of a signal following the selective inversion of another signal is monitored. Structural applications of T_1 measurements have been reviewed by Hall,[5] and applications of steady-state NOEs by Noggle and Schirmer,[6] and Bachers and Schaefer,[7] but the use of transient NOEs has received much less attention. However this technique offers several advantages.

The basic principle is that one signal is inverted by the application of a frequency selective pulse,[8] followed after a variable relaxation interval τ by a non-selective high-power pulse which monitors the partially relaxed intensity of all peaks. The enhanced spectra are thus acquired without instrumental and spectral perturbations arising from the continuous saturating radiofrequency field present in the steady-state NOE experiment. Furthermore, in steady-state NOE measurements, it is usually necessary to compare integrated intensities of enhanced and unenhanced spectra, since the saturating field also induces decoupling, hence changing peak multiplicities and/or linewidths. However, due to phase and baseline uncertainties it is difficult to measure integrated intensities sufficiently accurately to detect small (but perhaps structurally significant) NOEs of just a few percent. In the transient NOE technique on the other hand, since no decoupling occurs, quite small NOEs can readily be detected by comparing peak heights, provided care is taken to provide sufficient digital resolution. A coupled spectrum with NOE can be obtained by allowing the system to equilibrate under the influence of the saturating field and then gating the saturating field off immediately before data acquisition. However in using this technique on our spectrometer, we found it necessary to allow an instrumental recovery time of several tenths of a second between the gate and data acquisition. Since the steady-state NOE decays with time constant T_1 after removing the saturating field, its true magnitude may not be recorded accurately if the T_1 values are small. In contrast, a signal displaying a transient NOE reaches its maximum enhancement in a time of approximately T_1 following the selective inversion pulse.[3,4] A final advantage of the transient NOE technique is that two parameters characterise the effect, namely the maximum enhancement and the time of its occurrence.

Relaxation Theory and Method of Calculations.— Equations describing the coupled spin–lattice relaxation of an *N*-spin system have been set out by Noggle and Schirmer.[6] The relaxation of the longitudinal magnetisations S_i is governed by a set of N coupled differential equations (1) where S_i^0 represents the thermal

$$dS_i/dt = -\sum_j R_{ij}(S_j - S_j^0) \qquad (1)$$

equilibrium magnetisation and the sum runs over all nuclei. If all coupled spins are protons fixed in a rigid molecule and relaxing by their mutual dipolar interactions the relaxation coefficients (in the extreme nar-

rowing limit) are given by equations (2) and (3). r_{ij} Is the distance between nuclei i and j, τ_c is the correlation time for molecular tumbling (assumed isotropic), μ_o is the magnetic permeability of free space ($4\pi \times 10^{-7}$ H m^{-1}), and γ_H is the proton magnetogyric ratio. T_1^* Represents

$$R_{ii} = \left(\frac{\mu_o}{4\pi}\right)^2 \gamma_H^4 \hbar^2 \tau_c \sum_{j \neq i} \frac{1}{r_{ij}^6} + \frac{1}{T_1^*} \quad (2)$$

$$R_{ij} = \tfrac{1}{2}\left(\frac{\mu_o}{4\pi}\right)^2 \frac{\gamma_H^4 \hbar^2 \tau_c}{r_{ij}^6} \; (j \neq i) \quad (3)$$

the relaxation contribution from intermolecular interactions. If the internuclear vector is modulated by internal rotation as well as molecular tumbling, equation (2) and (3) are modified to take this into account. In the present case, the internal motion is rotation of the methyl group. Interactions affected are of two types, those between methyl protons and those between a methyl proton and a framework proton, H-15 and -19 being the most important. Rowan *et al.*[9] have given expressions for the case when one nucleus (i) is in a methyl group with three equilibrium positions and the other (j) is outside the methyl group but placed such that it is equidistant from two of the methyl protons. This treatment can readily be extended to the general case where the three possible i–j distances are all different. Denoting these distances by $r_{ij}^{(1)}$, $r_{ij}^{(2)}$, and $r_{ij}^{(3)}$, and letting $\beta_{ij}^{(ab)}$ be the angle between $r_{ij}^{(a)}$ and $r_{ij}^{(b)}$, we find that the quotients τ_c/r_{ij}^6 and τ_c/r_{ji}^6 in equations (2) and (3) are replaced by expression (4) with

$$\tfrac{1}{9}(A + 2B)\tau_c + 2(A - B)\,(\tau_c^{-1} + \tau_{int}^{-1})^{-1}] \quad (4)$$

$$A = \sum_{a=1}^{3} (r_{ij}^{(a)})^{-6} \text{ and } B = \sum_{a=1}^{2} \sum_{b>a} \tfrac{1}{2}(3\cos^2\beta_{ij}^{(ab)} - 1)(r_{ij}^{(a)} r_{ij}^{(b)})^{-3}$$

τ_{int} is the correlation time for internal rotation. If both i and j are methyl protons, then $r_{ij}^{(a)} = r_{ij}^{(b)} = r_{ij}^{(c)}$ and expression (4) simplifies to the expression given by Woessner *et al.*[10] for the situation where r_{ij} is invariant in magnitude to the internal rotation. In this case, τ_c in equations (2) and (3) is replaced by an effective correlation time given by equation (5) where α is the angle

$$\tau_c^{eff} = \tfrac{1}{4}(3\cos^2\alpha - 1)^2\tau_c + \tfrac{3}{4}(\sin^2 2\alpha + \sin^4\alpha)\,(\tau_c^{-1} + \tau_{int}^{-1})^{-1} \quad (5)$$

between r_{ij} and the axis of internal rotation.

The set of equations (1) can be written in matrix notation $d\bar{S}'/dt = -\bar{R}\bar{S}'$ where $\bar{S}'$ is a column vector with elements $S_i' = S_i - S_i^0$ and $\bar{R}$ is a relaxation matrix with elements R_{ij}. The solution of this equation is of the form (6) where $\bar{S}'(0)$ is the set of initial deviations from

$$\bar{S}'(t) = \exp(-\bar{R}t)\bar{S}'(0) \quad (6)$$

equilibrium. On substitution of values for correlation times and internuclear distances, the matrix exponential can be evaluated numerically to generate recovery curves for each nucleus. Effective spin–lattice relaxation times were calculated for all peaks in non-selective inversion experiments and for the inverted peak in selective inversion experiments from a least-squares fitting of a single exponential to the first 75% of the curve. The same procedure was used in reducing experimental recovery curves to a single characteristic parameter. Transient NOEs observed in selective inversion experiments are characterised by the maximum (or minimum) enhancement factor η^* and the time of its occurrence, t^*. η^* is defined by $\eta^* = \{S(t^*) - S^0\}/S^0$.

Steady-state NOEs were calculated from equations (1) by deleting the equation for the irradiated nucleus (k), and setting S_k and all derivatives in the remaining equations to zero. This leaves ($N - 1$) simultaneous equations (7). $\eta(j,k)$ Is the steady-state nuclear Overhauser

$$\sum_{k \neq j} R_{ij}\eta(j,k) = R_{ik} \; (i \neq k) \quad (7)$$

enhancement factor of nucleus j on irradiation of nucleus k. Since all nuclei are protons, then we have used the condition that S_i^0 is the same for all i. Equations (7) can be solved numerically on evaluation of the relaxation coefficients.

EXPERIMENTAL

Relaxation experiments were performed on a Varian Associates SC300 spectrometer operating at 300 MHz. Selective inversion experiments were carried out by pulsing the homonuclear decoupler. Π Pulse widths of *ca.* 20 ms were employed. Free induction decays were acquired into 32 K and these were weighted with an exponential function of time constant −1 s to reduce noise. To ensure that the thermal equilibrium magnetisations S_i° were measured accurately, pulse intervals of at least eight times the longest T_1 were employed

A solution of 1% in [$^2H_6$]acetone was used. The measurement temperature was 21 ± 1 °C.

RESULTS AND DISCUSSION

At 300 MHz, the ^1H n.m.r. spectrum of apparicine is completely resolved and almost first order. With two exceptions, initial assignments of the multiplets to protons on specific carbon atoms in the ring framework were made straightforwardly with the aid of spin-decoupling experiments and basic chemical shift and spin-spin coupling structure correlations. The exceptions are the aromatic pairs (H-9 and -12) and (H-10 and -11), the former both giving doublets at δ 7.29 and 7.39 and the latter triplets at δ 6.86 and 7.00.

These assignments, and the vital assignments of protons within the five non-equivalent methylene AB pairs on C-3, -6, -14, -17, and -21 were finally established (Table 1) by means of the spin–spin coupling constants and relaxation data presented in Tables 1—3. The AB pair protons are identified structurally in Figure 1. Note that the assignments of H-21a and 21b reported in ref. 1 are now reversed.

Before discussing the implications of this data with regard to the assignment of the AB pairs and to the molecular conformation, there are several other features of the relaxation data worth mentioning.

First, we note that there is a wide range of relaxation times, those of the aromatic protons being relatively long and those of the aliphatic methylene protons being relatively short. This disparity indicates that intra-

TABLE 1

^{1}H Chemical shifts (δ) and coupling constants (J/Hz) for apparicine in [$^2H_6$]acetone at 21 °C

Proton	δ	J
1	9.91	
3a	3.32	13.0 (3b), 7.9 (14a), 2.5 (14b)
3b	3.00	13.0 (3a), 11.2 (14a), 7.3 (14b), 1.5 (21b)
6a	4.42	18.0 (6b)
6b	3.98	18.0 (6a)
9	7.39	8.0 (10), 1.2 (11), 1.0 (12)
10	6.86	7.0 (11), 8.1 (9), 1.0 (12)
11	7.00	7.0 (10), 8.1 (12), 1.2 (9)
12	7.29	8.1 (11), 1.0 (9), 1.0 (10)
14a	2.13	13.6 (14b), 7.9 (3a), 11.2 (3b), 5.8 (15)
14b	1.85	13.6 (14a), 2.5 (3a), 7.3 (3b), 2.5 (15)
15	3.95	5.8 (14a), 2.5 (14b), 0.9 (18)
17a	5.59	
17b	5.30	
18	1.45	6.8 (19), 2.3 (21a), 0.9 (15), 0.9 (21b)
19	5.22	6.8 (18), 2.3 (21a)
21a	3.74	15.9 (21b), 2.3 (18), 2.3 (19)
21b	3.13	15.9 (21a), 0.9 (18), 1.5 (3b)

molecular interactions are the most important relaxation mechanism, since in general the aromatic proton relaxation is dominated by the *ortho*-interaction at *ca.* 250 pm, while the aliphatic methylene relaxation is dominated by the geminal interaction at *ca.* 180 p.m.

Secondly, over a period of days after making up the sample and making the first T_1 measurements, the NH signal was replaced by ^{2}H. This exchange was accompanied by significant increases of 20—30% in the T_1 values of the aromatic doublet at δ 7.29 and the olefinic singlet at δ 5.59 (Table 2). Since the magnetogyric ratio of ^{2}H is roughly one sixth that of ^{1}H, substitution by ^{2}H leads to a large reduction in the relaxation contribution from interactions with that nucleus. The observed enhancement of T_1 therefore permits the assignment of the doublet at δ 7.29 to H-12 and the singlet at δ 5.59 to H-17a, since these protons are closest to the NH. The remaining aromatic assignments follow from that of H-12.

Thirdly, there is a question of internal rotation of the methyl group. From equations (1), (2), (3), and (5), assuming only identical geminal interactions, it is predicted that for methyl rotation which is rapid compared to overall tumbling ($\tau_{int} \ll \tau_c$) a methyl ^{1}H T_1 is twice as large as the ^{1}H T_1 of a skeletal methylene. The observed methyl : average methylene ratio is 2.3, a difference which is readily explicable by the greater number of non-geminal interactions experienced by the skeletal methylenes. It has been assumed therefore that methyl rotation is extremely rapid, an assumption which more complete calculations of T_1s and NOEs have not challenged. As corroborative evidence, we note that the threefold barrier to methyl rotation in *cis*-but-2-ene is only 3.1 kJ mol^{-1} from microwave spectroscopy.[11] Using the approximate formula (8) where E_a is the methyl barrier, we

$$\tau_{int} \sim \frac{h}{kT} e^{Ea/RT} \quad (8)$$

obtain a value for τ_{int} of 6×10^{-13} s compared with the value of τ_c (see below) of 1.5×10^{-11} s.

Assignment of the AB methylene pairs is to a large extent unavoidably involved with the conformational analysis. The possible molecular conformations of apparicine can be separated into those of the (15-14-3-4-21-20-15) piperidine ring A and those of the (15-16-2-7-6-4-21-20-15) eight-membered ring B. These conformations were determined by verifying the consistency of experimental data on coupling constants (giving dihedral angles) and transient NOEs (giving information on proximate nuclei) with the limited number of stable conformations accessible to a Dreiding model of apparicine. The model conformations were those imposed purely by the geometrical constraints of bond lengths and angles. In view of the significance attached to fairly small transient NOEs in the following discussion, it seems desirable to show that such small effects can indeed be

TABLE 2

Effective spin–lattice relaxation times

Proton	Experimental [a]	Calculated [b]
1	3.38	3.33
3a	1.60	1.63
3b	1.55	1.47
6a	1.69	1.70
6b	1.60	1.66
9	6.07	6.48
10	6.20	6.42
11	6.90	6.60
12	8.85	8.65
	(11.75 [c])	(11.63 [c])
14a	1.42	1.30
14b	1.63	1.52
15	3.38	3.17
17a	1.71	1.81
	(2.07 [c])	(2.20 [c])
17b	1.65	1.65
18	3.68	3.53
19	5.5	4.46
21a	1.70	1.71
21b	1.50	1.55

[a] ±3%. [b] For details, see text. [c] Values in [1–^{2}H]-apparicine.

TABLE 3

Steady-state and transient nuclear Overhauser enhancements in [1-^{2}H]apparicine. Geminal NOEs are not included

Proton		η or η *		t */s	
Perturbed	Enhanced	Expt.[a]	Calc.[c]	Expt.[b]	Calc.[c]
6a	3b	0.04	0.033	2.5	2.3
	9	0.04	0.024	4.3	3.8
6b	9	0.03	0.024	4.3	3.8
	21b	0.04	0.031	2.7	2.7
9	6a	0.04	0.024	4.0	3.8
	6b	0.04	0.024	4.0	3.8
14a	3a	0.035	0.036	2.3	2.3
	15	0.05	0.043	2.0	2.3
	21a	0.04	0.039	2.0	2.3
14b	3b	0.03	0.038	2.9	2.3
	15	0.04	0.021	2.6	2.5
15	14a	0.04	0.040	2.0	2.6
	14b	0.02	0.019	2.0	2.4
	17a	−0.014	−0.010	~8	8.5
	17b	0.05	0.041	4.0	3.5
18	15	0.04	0.070	4.5	4.0
	19	0.075	0.089	4.8	4.7
18	15 [d]	0.15	0.13		
	19 [d]	0.20	0.18		
19	21b	0.04	0.063	4.0	3.6
21a	14a	0.02	0.04	2.9	2.2

[a] ±30%. [b] ±20%. [c] See text for details. [d] Steady-state enhancements, ±10%.

detected reliably. As an example therefore, Figure 2 shows the transient NOEs curves shown by the H-17 protons following selective inversion of H-15, together with the recovery curve of H-15. It is interesting to note that Figure 2 clearly shows that *negative* as well as *positive* transient NOEs can be observed. These are the dynamic counterpart of negative steady-state NOEs

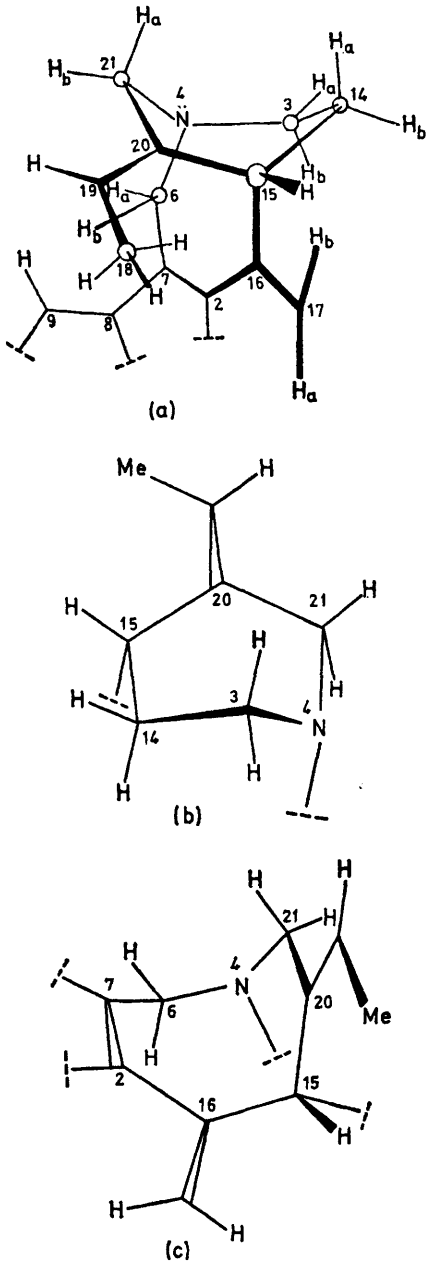

FIGURE 1 Dreiding model conformations of apparicine

arising in AMX spin systems when $r_{AX} > r_{AM}, r_{MX}$ and A (or X) is inverted.[6]

(i) *Conformation of Ring* A.—The significant items of experimental coupling constant and transient NOE data are these. (a) H-15 is coupled to the low-field H-14 with a moderate coupling of 5.8 Hz and to the high-field H-14 with a low coupling of 2.5 Hz. Since the stereochemistry of apparicine restricts the H-15–H-14 dihedral angles to the range 0—120°, the magnitude of these coupling constants indicates dihedral angles of *ca.* 45 and 75° between H-15 and the H-14 protons.[13] (b) Of the four couplings between the H-3 and -14 protons, three are relatively large at 7.3, 7.9, and 11.2 Hz, while only one is small at 2.5 Hz. Such a pattern can be obtained only for a C-3–C-14 conformation approaching eclipse of the C-15–C-14 and C-3–N-4 bonds. If the dihedral angle between the C-15–C-14 and C-3–N-4 bonds is 30°, giving H-3–H-14 dihedral angles of 30 (twice), 90, and 150°, the predicted J values [13] are 8.6, 2, and 10.4 Hz, respectively. (c) On selective inversion of H-19, a significant transient NOE is observed for the high-field H-21, but none for the low-field H-21. Hence H-19 is much closer to high-field H-21 than to the low-field. (d) On selective inversion of H-15, a larger transient NOE is observed for the low-field H-14 than for the high-field. (e) On selective inversion of

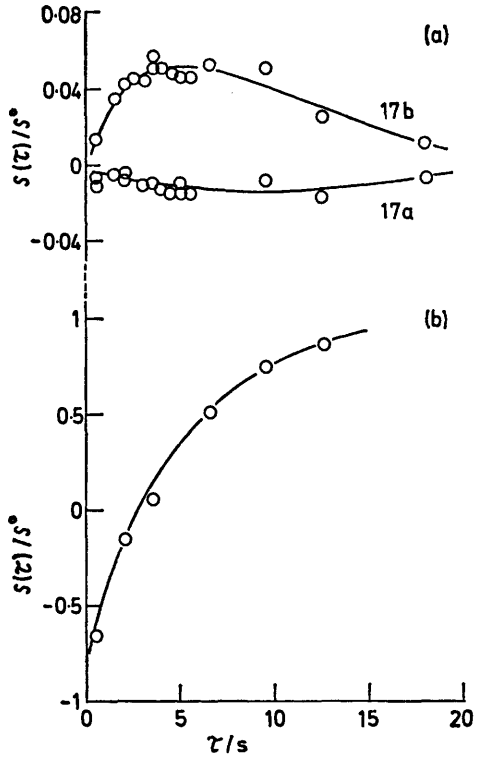

FIGURE 2 (a) Transient NOEs of H-17a and -17b on selective inversion of H-15. (b) Recovery curve of H-15 following selective inversion

the high-field H-14, the high-field H-3 shows a transient NOE whereas the low-field H-3 does not. Conversely, on selective inversion of the low-field H-14, the low-field H-3 shows a transient NOE whereas the high field does not. (f) On selective inversion of the H-14 or H-21 protons, there is a measurable interaction only between the low-field nuclei of both groups. (g) No transient NOEs are observed between the H-21 and H-3 protons.

These experimental data are consistent with the Dreiding model boat conformation shown in Figure 1(a)

and the peak assignments in Table 1. The model is slightly strained such that the dihedral angle between H-14a and -15 is *ca.* 45° and the dihedral angle between H-14a and -3a is *ca.* 30°. The H-21b C-21–C-20–C-19–H-19 fragment is almost planar. The alternative model conformation shown in Figure 1(b) is eliminated chiefly by the absence of any transient NOE between a H-21 proton and H-3 proton. Also it is impossible to reconcile all the experimental observations listed above with this conformation.

Two long-range couplings support the conformation in Figure 1(a). First, there is a four-bond coupling of 1.5 Hz between the high-field H-21 proton and the high-field H-3 proton. This is consistent with the assignment of H-21b and -3b and the almost planar zig-zag arrangement [14] of the H-21b–C-21–N-4–C-3–H-3b fragment in the proposed conformation. Secondly, there is a large allylic coupling of 2.3 Hz between the low-field H-21 and the methyl group. Both allylic and homoallylic couplings are relatively large in magnitude when the allylic C–H bond is at maximum inclination to the plane of the alkene.[15] Therefore the couplings observed are also consistent with the assignment and orientation of H-21a.

(ii) *Conformation Ring* B.—There are no coupling constants giving conformational data on this ring, but the transient NOE measurements do provide some reliable guidance on its structure. According to Dreiding models, ring B has two stable conformations with the C-16–C-17 double bond on either the same side [conformation I, Figure 1(a)] or on the opposite side [II, Figure 1(c)] of the indole plane as the 18-methyl group. In the models, the C-16–C-17 bond is inclined at an angle of 60—70° to the indole plane. Conformation I approximates the chair form and conformation II the boat form of cyclo-octane.[16] In conformation I, proton H-17b approaches the methyl group so closely that a steady-state NOE of 22% would be expected for H-17b on methyl irradiation, but no NOE is observed within experimental error. In conformation II, H-17b and -14a are proximate, but again there is no NOE evidence for any interaction. Furthermore, in both conformations the distance between H-1 and -17a is too great to be consistent with the large increase in the T_1 of H-17a on replacement of H-1 by ^{2}H. On substituting the experimental values of the relaxation time of H-17a with and without deuteriation of H-1 in expression (9) one obtains an

$$[T_1(17a, \text{apparicine})]^{-1} - \{T_1(17a, [1\text{-}^2H]\text{apparicine})\}^{-1} = \tfrac{3}{2}\left(\frac{\mu_0}{4\pi}\right)^2 \frac{\gamma_H^4 \hbar^2 \tau_c}{r_{1,17a}^6} \quad (9)$$

approximate value of 230 pm for $r_{1.17a}$. In contrast, $r_{1.17a}$ is >300 pm in both model conformations I and II. Thus it appears that the driving force of enhanced conjugation between the Π systems is strong enough to bring the C-16–C-17 double bond closer to the plane of the indole than molecular models would initially suggest. Indeed, the u.v. absorption spectrum of apparicine [2] is essentially that of a 2-vinylindole, indicating substantial conjugation.

TABLE 4

Interproton distances used to calculate relaxation parameters (pm)

Proton	1	3a	3b	6a	6b	9	10	11	12	14a	14b	15	17a	17b	18 [a]	19	21a	21b
1	—	*	*	*	*	*	*	*	273	*	462	404	239	347	*	500	*	*
3a		—	178	308	377	*	*	*	*	231	262	377	500	462	*	520	289	381
3b			—	239	316	500	*	*	*	285	231	416	345	345	*	520	354	389
6a				—	178	266	500	*	*	424	480	520	*	*	*	470	393	335
6b					—	266	500	*	*	424	520	480	*	*	*	308	347	243
9						—	244	429	494	*	*	*	*	*	*	*	*	*
10							—	248	429	*	*	*	*	*	*	*	*	*
11								—	248	*	*	*	*	*	*	*	*	*
12									—	*	*	*	520	*	*	*	*	*
14a										—	178	235	500	389	*	443	231	362
14b											—	258	366	270	*	530	362	466
15												—	354	243	273	370	335	408
17a													—	178	374	*	*	*
17b														—	339	*	*	*
18 [a]															231	270	*	*
19																—	335	231
21a																	—	178
21b																		—

* These distances are >500 pm and do not influence the relaxation behaviour.
[a] Effective distances, see text.

Interactions involving the H-6 protons provide further data on ring B. Experimentally, on selective inversion of H-9, both H-6 protons display almost equal transient NOEs. In model conformations I and II, one of the H-6 protons is close to H-9 (*ca.* 240 pm) and the other at a greater distance (*ca.* 360 pm). A differential transient NOE of the 6-H protons on inversion of H-9 is therefore expected if the molecule were fixed in either of these conformations. We note also significant transient NOEs from the H-6a–H-3b and H-6b–H-21b interactions, both of which are explicable by conformation II, but only the latter by conformation I.

The single conformation consistent with all these observations is a version of conformation II strained such that the C-16–C-17 bond lies at *ca.* 30° to the indole plane, and the indole plane bisects the H-6a–C-6–H-6b bond angle. It is still possible however that

this conformation represents an average between strained versions of conformations I and II. Our results are unable to distinguish between a single equilibrium state or exchange between two equilibrium states.

Calculations of Relaxation Times and NOEs.—Based on the previous discussion, trial values for internuclear distances were derived from a Dreiding model of apparicine constrained to occupy the conformation in Figure 1. The equilibrium positions of the methyl group were those with a methyl proton eclipsing the C-19–C-20 double bond.[11] In addition the C-18–C-19–C-20 bond angle was increased to 127°, the value obtaining [11] in *cis*-prop-2-ene. The C-20–C-19–H-19 bond angle was set at 118°.

The most reliable of these distances are those which affect the relaxation times of the H-10, -11, and -12 aromatic protons and the 3-, 14-, 17-, and 21-methylene groups. This set of eleven T_1 values was used to determine the optimum values of τ_c and T_1* in equations (2) and (3) by searching for the values giving a minimum in the quantity (10) *i.e.* minimising the squares of the

$$S = \sum_i \{(T_{1i}^{exp} - T_{1i}^{calc}/T_{1i}^{exp}\}^2 \qquad (10)$$

fractional deviation of the calculated effective relaxation times from the experimental values. This procedure gave the best-fit values τ_c 15.3 ± 1.0 ps and T_1* 35 ± 5 s, assuming errors of 2.5% in T_{1i}^{exp}. The remaining relaxation times, and the steady-state and transient NOEs were calculated using these values of τ_c and T_1*. Experimental and calculated parameters are compared in Tables 2 and 3. The matrix of internuclear distances is given in Table 4, principally for information, as it is not claimed that these distances are accurate to the precision quoted. Values given for interactions involving the methyl protons are effective distances taking into account the effect of methyl rotation, and are intended for direct substitution into equations (2) and (3) without modifying the correlation time. Transient NOEs were calculated for an average degree of inversion of 70%, obtained from an extrapolation of the recovery curve of the inverted signal.

Agreement between calculated and experimental parameters is quite satisfactory in view of the rather crude geometrical analysis, and indicates that the suggested conformation for apparicine is substantially correct. Great potential exists for the use of such n.m.r. relaxation techniques in solving similar conformational problems.

[9/984 *Received*, 25*th June*, 1979]

REFERENCES

[1] L. Akhter, R. T. Brown, and D. Moorcroft, *Tetrahedron Letters*, 1978, 4137.
[2] J. A. Joule, H. Monteiro, L. J. Durham, B. Gilbert, and C. Djerassi, *J. Chem. Soc.*, 1965, 1473.
[3] I. Solomon, *Phys. Rev.*, 1955, **99**, 559.
[4] I. Solomon and N. Bloembergen, *J. Chem. Phys.*, 1956, **25**, 261.
[5] L. D. Hall, *Chem. Soc. Rev.*, 1975, **4**, 401.
[6] J. H. Noggle and R. E. Schirmer, ' The Nuclear Overhauser Effect,' Academic Press, New York, 1971.
[7] G. E. Bachers and T. Schaefer, *Chem. Rev.*, 1971, **71**, 617.
[8] G. A. Morris and R. Freeman, *J. Magnetic Resonance*, 1978, **29**, 433.
[9] R. Rowan, J. A. McCammon, and B. D. Sykes, *J. Amer. Chem. Soc.*, 1974, **96**, 4773.
[10] D. E. Woessner, B. S. Snowden, and G. H. Meyer, *J. Chem. Phys.*, 1969, **59**, 719.
[11] K. Kondo, Y. Sakurai, E. Hirota, and Y. Morino, *J. Mol. Spectroscopy*, 1970, **34**, 231.
[12] R. Freeman, H. D. W. Hill, B. L. Tomlinson, and L. D. Hall, *J. Chem. Phys.*, 1974, **61**, 4466.
[13] Calculated from the Karplus equation $J(\phi) = 7 - \cos\theta + 5\cos 2\phi$ given by A. A. Bothner-By, *Adv. Magnetic Resonance*, 1965, **1**, 195. This equation was obtained empirically from coupling constant data for ethane and cyclohexane substituted with one or two electronegative groups.
[14] L. M. Jackman and S. Sternhell, 'Applications of Nuclear Magnetic Resonance Spectroscopy in Organic Chemistry,' Pergamon Press, Oxford, 1969, 2nd edn., p. 334.
[15] Ref. 14, pp. 316 and 325.
[16] E. L. Eliel, ' Stereochemistry of Carbon Compounds,' McGraw-Hill, New York, 1962.